Magnetic Resonance in Medicine 48:543–546 (2002)

Continuous Arterial Spin Labeling Using a Local Magnetic Field Gradient Coil

Robert Trampel,[1*] Toralf Mildner,[1] Ute Goerke,[1] Andreas Schaefer,[1] Wolfgang Driesel,[1] and David G. Norris[2]

Continuous arterial spin labeling (ASL) using a locally induced magnetic field gradient for adiabatic inversion of spins in the common carotid artery of human volunteers is demonstrated. The experimental setup consisted of a helmet resonator for imaging, a circular RF surface coil for labeling, and gradient loops to produce a magnetic field gradient. A spin-echo (SE) echo-planar imaging (EPI) sequence was used for imaging. The approach is independent of the gradients of the MR scanner. This technology may be used if the imaging gradient system does not produce an appropriate magnetic field gradient at the location of the carotid artery—for example, in a head-only scanner—and is a prerequisite for the development of a system that allows continuous labeling during the imaging experiment. Magn Reson Med 48:543–546, 2002. © 2002 Wiley-Liss, Inc.

Key words: arterial spin labeling; perfusion; adiabatic inversion; gradient coil; surface coil

Perfusion imaging using magnetically labeled water as an endogenous tracer is capable of measuring cerebral blood flow (CBF) (1–6). Continuous arterial spin labeling (CASL) can be achieved by RF irradiation in the presence of a magnetic field gradient along the carotid artery, which results in an adiabatic inversion of the flowing spins (1,7–9). In the past, separate labeling and imaging coils were used in animal experiments (8). A more recent development is their use in perfusion imaging in humans (9). The use of a dedicated RF transmission coil at the neck reduces power deposition and eliminates the need to correct for magnetization-transfer effects, thereby enabling multislice imaging (9). However, despite the potentially superior characteristics of perfusion-based activation studies compared to the conventionally used blood oxygenation level dependent (BOLD) contrast, they are seldom used. This is in part due to their inherently lower sensitivity and the longer acquisition time used. Compared with the numerous perfusion techniques available (1–6), CASL demonstrates a high sensitivity; however, for functional imaging, the temporal resolution is poor because of required labeling periods of several seconds prior to image acquisition. A possible means of increasing the temporal resolution in perfusion measurements was demonstrated by Silva et al. (10). If labeling could also be performed during image acquisition, the temporal resolution might be dramatically improved, enabling steady-state, multislice functional perfusion studies of the brain. This requires that the imaging and labeling experiments occur completely independently of each other.

In this work, independence of the labeling and imaging gradients is achieved by means of a separate local magnetic field gradient coil for adiabatic inversion at the neck. A locally induced magnetic field gradient combined with separate RF coils for both labeling and imaging is a first step toward true continuous labeling—that is, even during image acquisition.

METHODS

All experiments were performed using a 3-T whole-body MR scanner (Bruker Medical, Ettlingen, Germany). A sketch of the custom-built experimental setup consisting of the local magnetic field gradient coil (the "gradient module") and an RF single-loop surface coil is shown in Fig. 1. The gradient module consisted of two loops with four windings each. The distance between the two loops was 7 cm. Other dimensions are given in Fig. 1. A circular RF coil was placed within the gradient module. Because the human common carotid artery is located at a maximum depth of about 3 cm, a diameter of 6 cm was chosen for the RF coil to guarantee sufficient RF power at the position of the artery. Both the RF coil and the gradient module were packed into an ergonomically-shaped plastic box that allowed a good fit to the neck.

The magnetic field gradient produced by the gradient module was determined with nonlocalized proton NMR spectroscopy using a water phantom, which consisted of four equidistant containers along the z-axis of the gradient module and was placed at a distance of 3 cm at the expected location of the carotid artery (Fig. 1). Due to the presence of the gradient the spectrum consisted of four single lines, and the gradient strength was easily obtained from the frequency separation of the peaks and the known distance between the water containers. The gradient module was found to generate a gradient field of about 0.5 mT m^{-1} A^{-1}. The exact magnetic field profile between the kidney-shaped gradient loops was measured outside the main magnetic field of the MR scanner using a pickup coil, which was placed at a distance of 3 cm above the gradient module (expected location of the carotid artery). An alternating current of low amplitude induced a voltage in the pickup coil, which is linearly related to the amplitude of the magnetic field. Figure 2 shows the variation of magnetic field strength as a function of the position of the pickup coil. As a result, the gradient module produced a fairly constant magnetic field gradient at the expected location of the carotid artery.

The gradient strength needed for inversion, and the inversion efficiency α were determined by measurements

[1]Max Planck Institute of Cognitive Neuroscience, Leipzig, Germany.
[2]F.C. Donders Center for Cognitive Neuroimaging, Nijmegen, The Netherlands.
*Correspondence to: R. Trampel, Max Planck Institute of Cognitive Neuroscience, Stephanstr. 1a, 04103 Leipzig, Germany. E-mail: trampel@cns.mpg.de
Received 11 January 2002; revised 15 April 2002; accepted 19 April 2002.
DOI 10.1002/mrm.10228
Published online in Wiley InterScience (www.interscience.wiley.com).

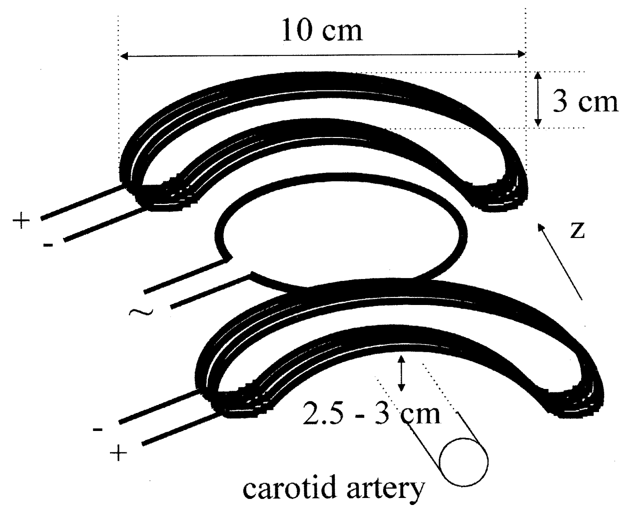

FIG. 1. Sketch of the circular RF surface coil combined with the kidney-shaped gradient module.

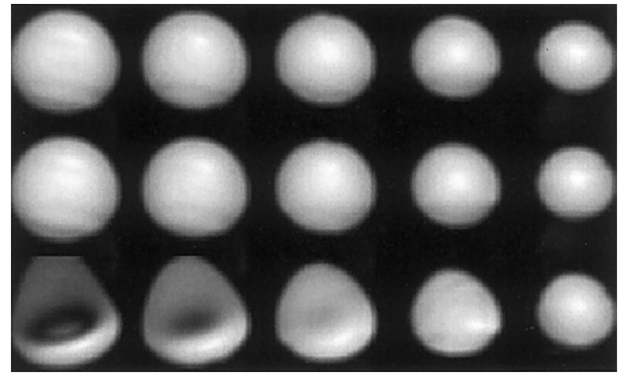

FIG. 3. Images recorded without a current in the local magnetic field gradient coil (top row) and in the presence of the locally-induced magnetic field gradient (middle row). The images of the top and middle row were acquired at a distance of 25–30 cm from the center of the gradient module. The images of the bottom row were obtained in the presence of the magnetic field gradient at a distance of 10–15 cm from the center of the gradient module.

with a flow phantom. It consisted of a flexible tube, a lowered and an elevated reservoir to enable a constant flow, a valve to adjust the flow velocity, and a pump, which pumped the water from the lowered to the elevated reservoir. The mean flow in the tube was adjusted to a velocity of 40 cm s^{-1} to match typical conditions in the human common carotid artery. The labeling coil (consisting of the RF surface coil and the gradient module) was placed 3 cm above the tube. After a labeling period, which was sufficiently long to ensure that the sampled length of the tube was filled with labeled water, a set of 13 axial slices (slice gap = 1.5 cm, slice thickness = 0.5 cm) was acquired with a spin-echo (SE) EPI sequence (TE = 22 ms, echo position at 40% of the echo train length, acquisition bandwidth = 100 kHz) using a birdcage resonator. The distance between the center slice and the labeling coil was 25 cm. Subsequently, an identical set of slices was acquired using the same technique but without labeling. The magnetization ratio with and without labeling, $M_z/M_{z,0}$, directly after passing the labeling coil was determined by extrapolating a T_1 fit of the course of the magnetization ratios of the 13 slices. The inversion efficiency was then calculated as $\alpha = (1 - M_z/M_{z,0})/2$. Gradient strengths of 1.5–2 mT m^{-1} repeatedly yielded an inversion efficiency above 90% at an RF power level of 0.4 W. No torque effects were detected for the corresponding currents in the gradient module between 3 and 4 A. Based on the calibration results, a gradient of 2 mT m^{-1} was chosen for all in vivo experiments.

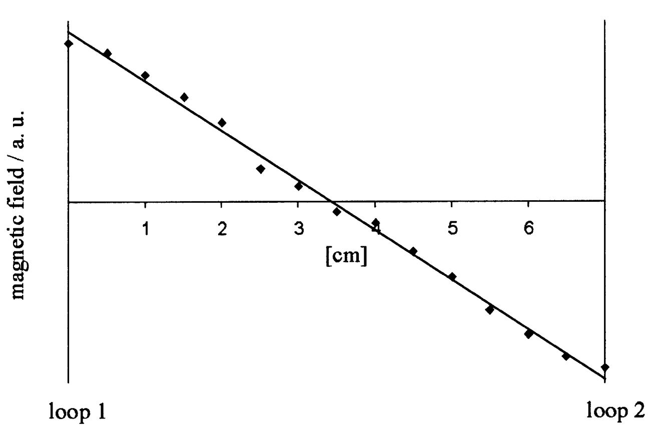

FIG. 2. Plot of the magnetic field between the two gradient loops at a distance of 3 cm from the plane of the RF coil. The solid line is the result of a linear fit.

Potential image distortions due to the locally induced magnetic field gradient were examined using a spherical gel phantom with a diameter of 16 cm. An SE-EPI sequence (TE = 22 ms, echo position at 40% of the echo train length, acquisition bandwidth 100 kHz) with a repetition time (TR) of 8 s was used for imaging. The field of view (FOV) was 19.2 cm, and the in-plane pixel size was 0.3 cm × 0.3 cm. The images were acquired using a custom-built helmet resonator (11). Thus the same parameters were used as for the in vivo experiments. Three sets of five axial slices (slice gap = 0.8 cm, slice thickness = 0.5 cm) were acquired and are shown in Fig. 3. The images in the first set were obtained in the absence of the locally-induced magnetic field gradient. In the second set, image acquisition was performed after reshimming with the current in the gradient module switched on. For both sets of images the center of the gradient module was placed at a distance of 25 cm from the closest slice. The effect of the proximity of the gradient module to the helmet resonator can be seen in the third set of images acquired with a minimum distance of only 10 cm between the gradient module and the closest slice. Only the uppermost image is undistorted. As this was positioned about 15 cm from the center of the gradient set, separations smaller than 16 cm were not used in subsequent in vivo experiments.

To demonstrate the feasibility of perfusion imaging, two healthy human volunteers (26 and 33 years old) were examined. Both gave informed written consent. For the in vivo studies, the custom-built helmet resonator (11) was used. Anatomical images were obtained with a T_1-weighted modified driven equilibrium Fourier transform

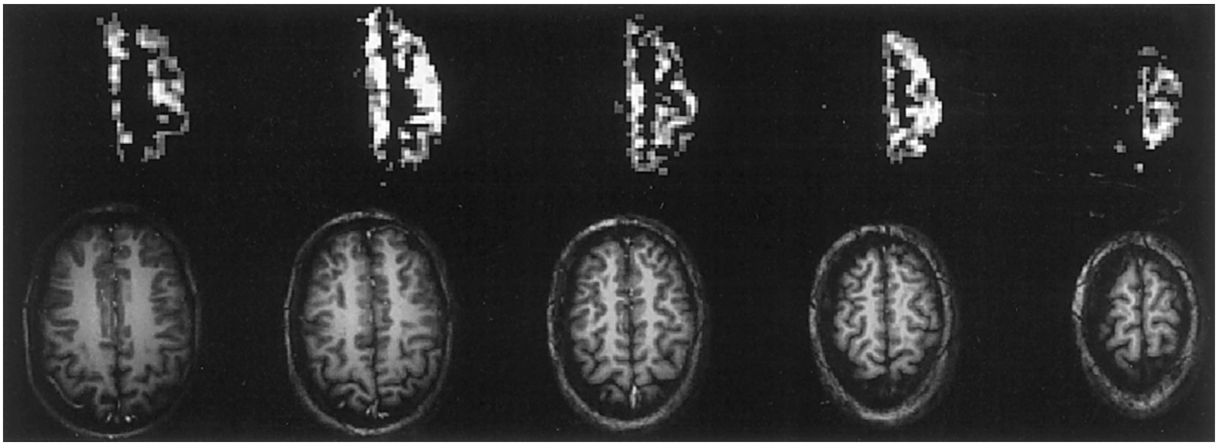

FIG. 4. Top: Images of the signal difference between the conditions of ASL and no labeling. Bottom: T_1-weighted anatomical images.

(MDEFT) sequence (12). An SE-EPI sequence with identical parameters as for the distortion tests was used for functional imaging. Refocusing the magnetization as an SE was favored over more conventionally used gradient-echo EPI techniques to reduce the sensitivity to magnetic field heterogeneities (i.e., T_2^* effects). Five axial slices (slice gap = 0.2 cm, slice thickness = 0.5 cm, FOV = 19.2 cm, pixel size = 0.3 cm × 0.3 cm) were acquired at a distance of about 25 cm between the center of the gradient module and the closest slice. A total of 140 repetitions were recorded with a TR of 8 s. Each repetition included a labeling period of 4 s and a post-label delay of 2 s (13). For control measurements, RF irradiation in the RF surface coil was omitted during even repetitions; that is, images with ASL and control scans without labeling were recorded in an interleaved fashion. The long TR of 8 s was used to facilitate quantification without consideration of residual effects from preceding spin-labeling periods in the control data. The RF power absorption during the labeling period was about 0.4 W. The current in the gradient module remained switched on during the whole experiment, including shimming prior to the perfusion experiment. The frequency of the labeling pulse was set on resonance with respect to the magnetic field at the center of the labeling coil. No additional detuning of the RF surface coil was necessary during image acquisition.

RESULTS

The signal difference between the conditions of ASL and no labeling is depicted in Fig. 4. The RF coil and gradient module were placed over the right carotid artery of the subject. A significant difference between the two conditions was obtained only for the right hemisphere. The vanishing signal differences in the contralateral hemisphere indicate the absence of magnetization transfer effects, as argued previously (9). The highest sensitivity to ASL was observed in gray matter, as indicated by comparison of the top and bottom rows of Fig. 4. The lower sensitivity of white matter can be explained by the shorter T_1 and the lower values of the CBF compared to gray matter. For an estimation of the sensitivity, we refer to Eq. [3] from Ref. 13. The percentage signal change $\Delta M_z/M_{z,0}$ obtained for gray matter was between −0.5% and −1.3%, where ΔM_z is the difference of the magnetization with and without labeling, and $M_{z,0}$ is the magnetization of the control image. This corresponds to CBF values of 50–150 ml/min/100 g, which were obtained by use of Eq. [3] of Ref. 13. The T_1 in gray matter and arterial blood are within 10% of each other at 3 Tesla (about 1.3 s), so the transit-time sensitivity was neglected (13). The brain–blood partition coefficient λ was assumed to be 0.9 (14,15), and the inversion efficiency α to be 0.9. The post-label delay was 2 s.

DISCUSSION

The values of the CBF obtained with our experimental setup are in a reasonable physiological range (16). Two potential errors for the quantification of the CBF were reduced by recent techniques (9,13). First, magnetization transfer was eliminated using separate labeling and imaging coils (9). Second, the influence of the arterial transit time was minimized by the long post-label delay (13).

The method introduced in this work utilizes two gradient loops and an RF coil, both separated from the imaging coil. It was shown that the locally induced magnetic field gradient does not influence the SE-EPI images, provided a minimum distance between the gradient module and the imaging coil is maintained. Thus, the locally-induced magnetic field gradient should allow true continuous labeling even during image acquisition. However, two problems still need to be addressed. First, although the B_1 field at the helmet coil arising from the RF surface coil is too small to cause magnetization transfer effects, it is still possible that this interferes with the signal acquisition. This was the case with our current experimental setup, and thus image acquisition during the application of the RF labeling pulse was not possible. Second, the gradient fields used for imaging may overlay the local inversion gradient, influencing the inversion efficiency. This problem has not yet been investigated. The elimination of these effects is an area of ongoing research and was beyond the scope of this feasibility study.

In scanners equipped solely with head-only gradient systems, the gradient field at the neck may be inadequate for CASL and, hence, the realization of an independent gradient coil may provide the only means of implementing this technique even for resting state measurements of perfusion. Further development should minimize the size of the gradient module and enable the use of gradient modules at both carotid arteries.

In conclusion, in vivo experiments demonstrated ASL with a gradient module that was placed directly over the carotid artery of two human volunteers. The method has the potential to achieve true continuous spin labeling even during image acquisition, and will be necessary for ASL at the neck if the system's own gradients cannot produce a suitable magnetic field gradient at the carotid artery.

ACKNOWLEDGMENTS

The authors thank Harald Möller, Christopher J. Wiggins, and Manfred Weder for advice and technical assistance. Anke Mempel, Mandy Naumann, Claudia Buschendorf, and Reiner Hertwig are thanked for logistical support.

REFERENCES

1. Williams DS, Detre JA, Leigh JS, Koretsky AP. Magnetic resonance imaging of perfusion using spin inversion of arterial water. Proc Natl Acad Sci USA 1992;89:212–216.
2. Detre JA, Leigh JS, Williams DS, Koretsky AP. Perfusion imaging. Magn Reson Med 1992;23:37–45.
3. Edelman RR, Siewert B, Darby DG, Thangaraj V, Nobre AC, Mesulam MM, Warach S. Qualitative mapping of cerebral blood flow and functional localization with echo-planar MR imaging and signal targeting with alternating radio frequency. Radiology 1994;192:513–520.
4. Kwong KK, Chesler DA, Weisskoff RM, Donahue KM, Davis TL, Ostergaard L, Campbell TA, Rosen BR. MR perfusion studies with T1-weighted echo-planar imaging. Magn Reson Med 1995;34:878–887.
5. Kim SG. Quantification of relative cerebral blood flow change by flow-sensitive alternating inversion recovery (FAIR) technique: application to functional mapping. Magn Reson Med 1995;34:293–301.
6. Schwarzbauer C, Morrissey SP, Haase A. Quantitative magnetic resonance imaging of perfusion using magnetic labeling of water proton spins within the detection slice. Magn Reson Med 1996;35:540–546.
7. Dixon WT, Du LN, Faul DD, Gado M, Rossnick S. Projection angiograms of blood labeled by adiabatic fast passage. Magn Reson Med 1986;3:454–462.
8. Zhang W, Silva AC, Williams DS, Koretsky AP. NMR measurement of perfusion using arterial spin labeling without saturation of macromolecular spins. Magn Reson Med 1995;33:370–376.
9. Zaharchuk G, Ledden PJ, Kwong KK, Reese TG, Rosen BR, Wald LL. Multislice perfusion and perfusion territory imaging in humans with separate label and image coils. Magn Reson Med 1999;41:1093–1098.
10. Silva AC, Kim SG. Pseudo-continuous arterial spin labeling technique for measuring CBF dynamics with high temporal resolution. Magn Reson Med 1999;42:425–429.
11. Merkle H, Driesel W, Andersen P, Adriany G, Ugurbil K, Garwood M. Circularly polarized RF helmet coil for brain studies at 7 Tesla. In: Proceedings of the 8th Annual Meeting of ISMRM, Denver, 2000. p 565.
12. Norris DG. Reduced power multislice MDEFT imaging. J Magn Reson Imaging 2000;11:445–451.
13. Alsop DC, Detre JA. Reduced transit time sensitivity in noninvasive magnetic resonance imaging of human cerebral blood flow. J Cereb Blood Flow Metab 1996;16:1236–1249.
14. Iida H, Kanno I, Miura S, Murakami M, Takahashi K, Uemura K. A determination of the regional brain/blood partition coefficient of water using dynamic positron emission tomography. J Cereb Blood Flow Metab 1989;9:874–885.
15. Herscovitch P, Raichle ME. What is the correct value for the brain-blood coefficient for water? J Cereb Blood Flow Metab 1985;5:65–69.
16. Calamante F, Thomas DL, Pell GS, Wiersma J, Turner R. Measuring cerebral blood flow using magnetic resonance imaging techniques. J Cereb Blood Flow Metab 1999;19:701–735.